Journal of Alloys and Compounds 509 (2011) 7175–7180

Contents lists available at ScienceDirect

Journal of Alloys and Compounds

journal homepage: www.elsevier.com/locate/jallcom

Effect of SnO_2 doping on microstructural and electrical properties of ZnO–Pr_6O_{11} based varistor ceramics

Hai Feng[a], Zhijian Peng[a,*], Xiuli Fu[b,*], Zhiqiang Fu[a], Chengbiao Wang[a], Longhao Qi[c], Hezhuo Miao[c]

[a] School of Engineering and Technology, China University of Geosciences, Beijing 100083, PR China
[b] School of Science, Beijing University of Posts and Telecommunications, Beijing 100876, PR China
[c] State Key Lab of New Ceramics and Fine Processing, Tsinghua University, Beijing 100084, PR China

ARTICLE INFO

Article history:
Received 23 December 2010
Received in revised form 2 April 2011
Accepted 5 April 2011
Available online 12 April 2011

PACS:
84.32.Ff
61.72.–y

Keywords:
ZnO varistor
Pr_6O_{11}
SnO_2 doping
Electrical properties

ABSTRACT

ZnO–Pr_6O_{11} based varistor ceramics doped with 0–2.0 mol% SnO_2 were fabricated by sintering samples at 1300 °C for 2 h with conventional ceramic processing method. X-ray diffraction analysis indicated that the doped SnO_2 reacted with praseodymium oxides during sintering, generating $Pr_2Sn_2O_7$ phase. Through scanning electron microscopy, it was found that the doping of SnO_2 played a role against the growth of ZnO grains. Capacitance–voltage analysis revealed that the doped SnO_2 acted as a donor in the varistor. The measured electric-field/current-density characteristics of the samples showed that the varistor voltage increased with the increase of SnO_2 doping content, when the SnO_2 content was no more than 1.0 mol%; with the SnO_2 content up to no more than 0.5 mol%, the doping of SnO_2 could increase the nonlinear coefficient; but, when the SnO_2 doping content was further increased, the nonlinear coefficient and varistor voltage of the samples decreased, and the leakage current increased.

1. Introduction

ZnO varistors are electronic ceramic devices produced by sintering ZnO powder with small amounts of various metal oxides. They exhibit highly nonlinear current–voltage (I–V) characteristics expressed by $I = kV^{\alpha}$, where k is a constant, and α is the nonlinear coefficient, an inherent parameter of varistors. Because of their high nonlinearity, they have been used to sense and limit transient voltage surges, both in ac and dc fields and over a wide range of voltages. Today ZnO varistors are being extensively applied to protect various semiconductor devices and electric power systems [1–3].

Although the main composition of ZnO varistor materials is ZnO, ZnO itself does not exhibit nonlinear I–V characteristics. It is the dopants of Bi_2O_3, Pr_6O_{11}, or such alike that impart them the non-ohmic property, which are known as varistor-forming oxide (VFO) [3,4]. Literature even classifies ZnO varistors into ZnO–Bi_2O_3 based varistors, ZnO–Pr_6O_{11} varistors, and so on, on the basis of the key material VFO in them.

Now the most commercially used ZnO varistors are ZnO–Bi_2O_3 based. However, although ZnO–Bi_2O_3 based varistors exhibit excellent varistor properties, they have a few drawbacks, due to the high volatility and reactivity of Bi_2O_3 during liquid sintering [5]. To overcome these problems, various ZnO varistors with new VFOs, such as ZnO–Pr_6O_{11} based varistors, have been studied actively [6]. Compared with ZnO–Bi_2O_3 based varistors, ZnO–Pr_6O_{11} based ceramic varistors have a simple two-phase microstructure of ZnO grain and a Pr oxide intergranular phase which can increase the active grain boundary area through which electrical current flows [7,8].

ZnO ceramics containing Pr_6O_{11} and Co_3O_4 exhibiting non-ohmic current characteristics were first reported by Mukae [7]. From then on, lots of literatures about ZnO–Pr_6O_{11} based varistors have been published, in which the doping effects of rare earth metal oxides such as Er_2O_3, Y_2O_3, Dy_2O_3 and La_2O_3, or other metal oxides such as MnO_2, Sb_2O_3, TiO_2 and Fe_2O_3 on the microstructural and electrical properties of ZnO–Pr_6O_{11} based varistors have been well studied [9–20]. It was found that the doping of appropriate amount of Y_2O_3, Er_2O_3, Dy_2O_3, TiO_2 or Fe_2O_3 could improve the nonlinear properties of ZnO–Pr_6O_{11} based varistors [9,13,14,17,18,20]. Compared with ZnO–Bi_2O_3 based varistors, in which the doping effects of most additives have been well studied [21–26], however, the doping effects of many additives on ZnO–Pr_6O_{11} based varistors have been still not clear yet. Some promising additives, such as SnO_2, which were commonly found in the well-studied ZnO–Bi_2O_3 system are not reported in ZnO–Pr_6O_{11} system.

In ZnO–Bi_2O_3 based varistors, it was reported that the replacement of ZnO by appropriate amount of SnO_2 could increase the nonlinear exponents of samples [27–29]. But in ZnO–Pr_6O_{11} based

* Corresponding authors. Tel.: +86 10 82320255; fax: +86 10 82322624.
E-mail addresses: pengzhijian@cugb.edu.cn (Z. Peng), xiulifu@bupt.edu.cn (X. Fu).

0925-8388/$ – see front matter © 2011 Elsevier B.V. All rights reserved.
doi:10.1016/j.jallcom.2011.04.042

varistors, there is no literature about how the varistor properties change when ZnO is substituted by SnO_2. So, in this work, we systematically replaced the portion of ZnO in ZnO–Pr_6O_{11} based varistors with different amounts of SnO_2 so as to investigate the effect of SnO_2 doping on the microstructural and electrical properties of ZnO–Pr_6O_{11} based ceramic varistors.

2. Experimental procedures

2.1. Sample preparation

Samples with a nominal composition of $(98.0-x)$ mol% ZnO + 0.5 mol% Pr_6O_{11} + 1.0 mol% Co_3O_4 + 0.5 mol% Cr_2O_3 + x mol% SnO_2 (x = 0.0, 0.25, 0.5, 1.0, 2.0) were fabricated using a conventional ceramic processing method [30,31]. All the raw materials are commercially bought powders of reagent grade. For the sample of each composition, the raw powders were mixed and ball-milled in de-ionized water for at least 24 h. Then the resultant slurries were dried in air at 120 °C. After drying, the chunks of powder mixture were crashed into fine powders and sieved. After that, the powders were pressed into discs of 6 mm in diameter and 1.5 mm in thickness with a pressure of 40 MPa, and then the green samples were sintered in a muffle oven at 1300 °C in air for 2 h with heating rate of 2 °C/min and cooling naturally. In order to measure the electrical properties, silver pastes were coated and toasted on both sides of the sintered samples.

2.2. Materials characterization

The sample diameter shrinkage was calculated in the percentage of the diameter difference between the green body and sintered one. The apparent density (ρ) of the as-prepared samples was measured by Archimedes method according to international standard (ISO18754), and the relative density was calculated in the percentage of the average apparent density to theoretical density. The phase composition of the samples was identified by X-ray diffractometer (XRD, D/max2550HB+/PC, Cu Kα, and λ=1.5418 Å) using a continuous scanning mode with speed of 8°/min. To investigate the microstructures of the samples, either of the sample surfaces was lapped and ground with SiC paper, and polished with 0.3 μm Al_2O_3 powder paste to a mirror-like surface. The polished samples were then thermally etched at 1100 °C for 30 min. Then the etched surface was examined via a scanning electron microscope (SEM, Model: SSX-550) equipped with an energy dispersive X-ray spectroscopy (EDS). The ZnO grain size (d) of the samples was determined from the SEM images using linear intercept method.

The capacitance–voltage (C–V) characteristics of the as-prepared varistor ceramics were measured at 1 kHz using keithley 4200-SCS recorder. The donor density (N_d) of ZnO grains and the barrier height (Φ_b) at the grain boundary were determined from the following equation proposed by Mukae et al. [32].

$$\left(\frac{1}{C}-\frac{1}{2C_0}\right)^2=\frac{2t}{A^2de\varepsilon N_d}V+\frac{2t^2}{A^2d^2e\varepsilon N_d}\phi_b \quad (1)$$

where C_0 and C are the corresponding capacitances of the samples under different applied voltages, in which C_0 is the value of C when V = 0, and V is the applied voltage; t is the thickness of the specimens, A is the electrode area of the specimens, and d is the average grain size; and ε is the permittivity of ZnO, and e is electron charge.

The electric field vs current density (E–J) characteristics of the samples were recorded at room temperature with a high-voltage source measurement unit (Model: CJ1001). The varistor voltage (V_B) was determined at 1 mA/cm^2 and the leakage current (I_L) was determined at 0.75 V_B. Moreover, the nonlinear coefficient (α) was calculated using

$$\alpha=\frac{\log(J_2/J_1)}{\log(E_2/E_1)}=\frac{1}{\log(E_2/E_1)} \quad (2)$$

where E_1 and E_2 are the electric fields corresponding to J_1 = 1 mA/cm^2 and J_2 = 10 mA/cm^2, respectively.

The applied voltage per grain boundary (V_{gb}) was calculated using

$$V_{gb}=V_B\cdot\frac{d}{D} \quad (3)$$

where V_B is the varistor voltage of the ceramic varistors, d is the average size of ZnO grains, and D is the thickness of the sintered samples.

3. Results and discussion

3.1. Sinterabilities

Fig. 1 illustrates the diameter shrinkage of the as-prepared samples doped with different amounts of SnO_2. It can be easily seen that the diameter shrinkage decreases with the increase of SnO_2 doping contents, indicating the samples shrink less with more SnO_2 doped. In particular, when the doping content of SnO_2 is more than 0.5 mol%, the diameter shrinkages of the samples decrease more quickly. So, it can be deduced that the doping of SnO_2 plays a role against the sintering of ZnO–Pr_6O_{11} based varistor ceramics. Fig. 2 shows the apparent densities (also listed in Table 1) and relative densities of the ZnO–Pr_6O_{11} based varistor ceramics doped with different amounts of SnO_2. The apparent density increases as the doping amount of SnO_2 increases up to 0.5 mol%, which might be mainly due to the higher density of SnO_2 (6.995 g/cm^3) than that of ZnO (5.672 g/cm^3), and the little increase of relative density. With further increase of SnO_2 doping contents, the apparent density of the samples decreases abruptly, which is consistent with the quick decreases in diameter shrinkage and relative density. So, it can be concluded that although the doping of SnO_2 plays a role against the sintering of ZnO–Pr_6O_{11} based varistor ceramics, one can still make denser samples with the doping amount of SnO_2 up to 0.5 mol%,

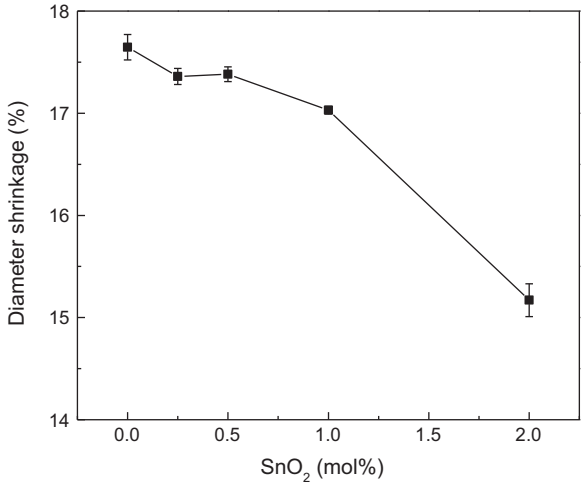

Fig. 1. The diameter shrinkages of the as-prepared ZnO–Pr_6O_{11} based varistor ceramics doped with different amounts of SnO_2.

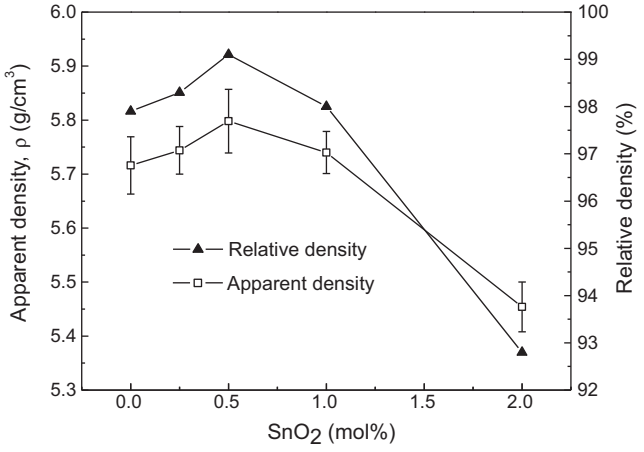

Fig. 2. The apparent densities and relative densities of the as-prepared ZnO–Pr_6O_{11} based varistor ceramics doped with different amounts of SnO_2.

Table 1
Microstructural and electrical parameters of the as-prepared ZnO–Pr_6O_{11} based ceramic varistors doped with different amounts of SnO_2.

Doping amount of SnO_2 (mol%)	ρ (g/cm^3)	d (μm)	$V_{1\,mA}$ (V/mm)	α	I_L (μA)	V_{gb} (V)
0.0	5.716	9.02	340	10.9	23	3.07
0.25	5.744	8.42	398	19.8	18	3.35
0.5	5.798	7.26	537	24.5	14	3.89
1.0	5.74	2.1	642	11.1	140	1.35
2.0	5.454	1.1	336	2.8	710	0.37

which is very important in obtaining high-performance ceramic varistors.

3.2. Composition and microstructure

Fig. 3 displays the XRD patterns of the as-prepared ZnO–Pr_6O_{11} based varistor ceramics doped with different amounts of SnO_2, in which the intensities of all the diffraction peaks are normalized. From this figure, it can be seen that the phase composition of the sample without SnO_2 are ZnO and Pr_6O_{11} phases. With increasing doping amount of SnO_2 up to 0.5 mol%, there is no new phase detected, but the peak intensities of Pr_6O_{11} phase decrease gradually. When the doping amount of SnO_2 was more than 0.5 mol%, a new phase, $Pr_2Sn_2O_7$, was detected in the samples, and Pr_6O_{11} phase could even not be detected within XRD limits. So, it can be concluded that the doped SnO_2 would react with Pr_6O_{11} during the sintering, generating $Pr_2Sn_2O_7$.

Fig. 4 presents typical SEM images of the as-prepared ZnO–Pr_6O_{11} based varistor ceramics doped with different amounts of SnO_2. It is well known that the microstructure of ZnO–Pr_6O_{11}

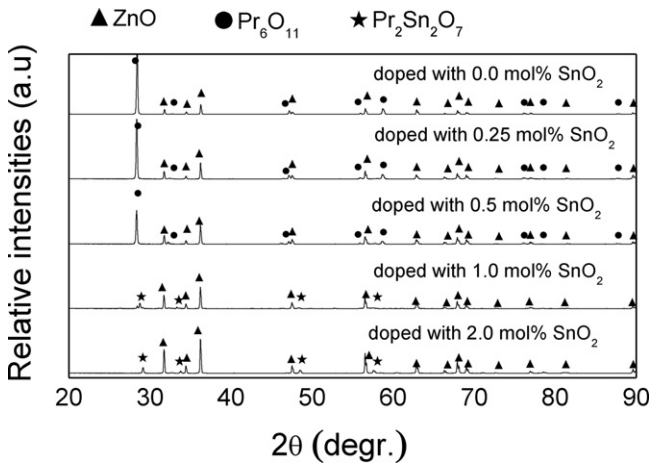

Fig. 3. XRD patterns of the as-prepared ZnO–Pr_6O_{11} based varistor ceramics doped with different amounts of SnO_2.

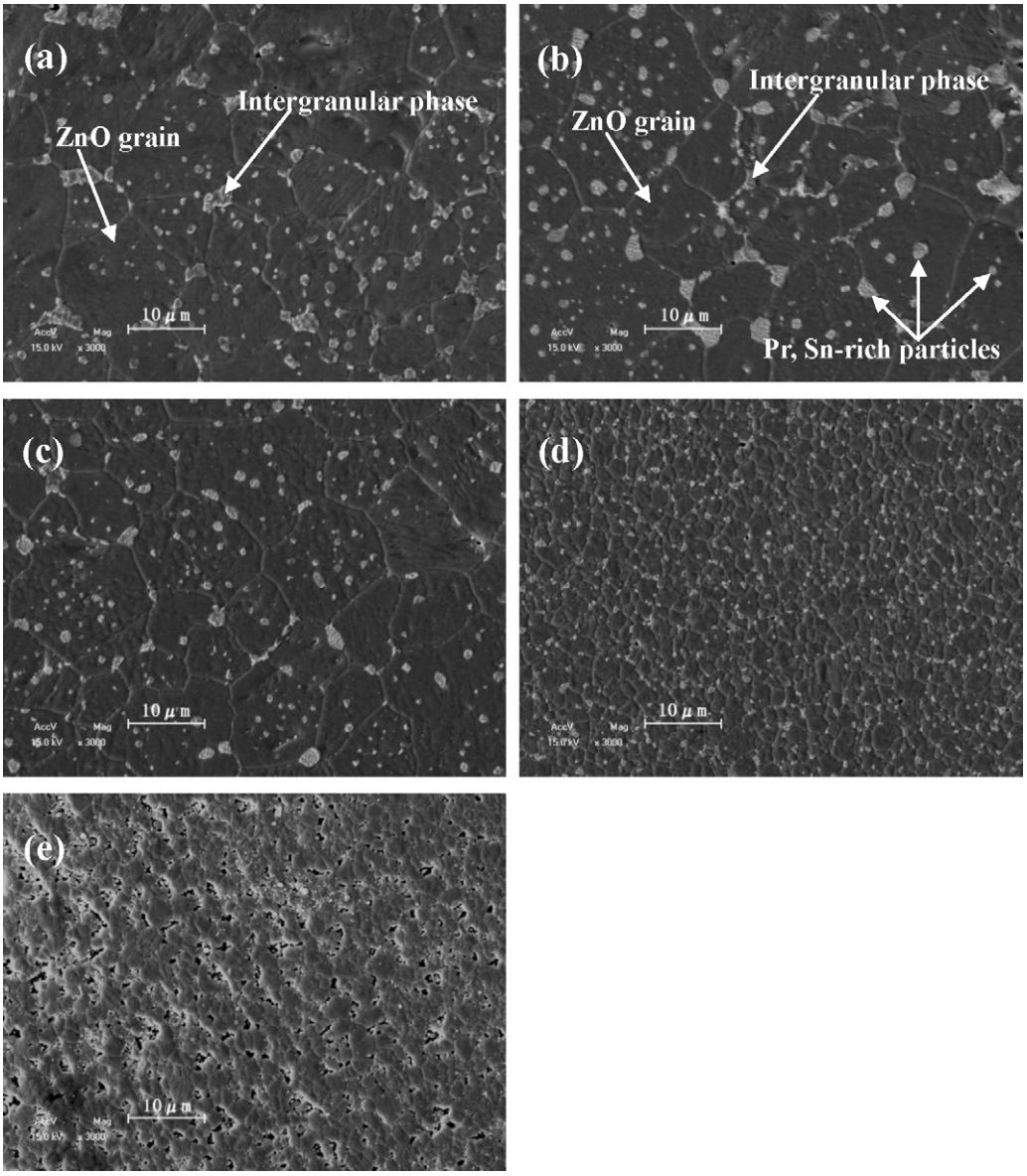

Fig. 4. Typical SEM images of the as-prepared ZnO–Pr_6O_{11} based varistor ceramics doped with different amounts of SnO_2: (a) 0.0 mol% SnO_2, (b) 0.25 mol% SnO_2, (c) 0.5 mol% SnO_2, (d) 1.0 mol% SnO_2 and (e) 2.0 mol% SnO_2.

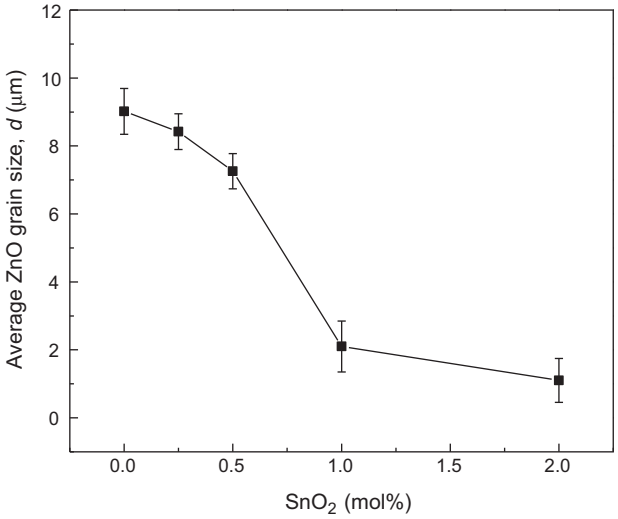

Fig. 5. The average ZnO grain sizes of the as-prepared ZnO–Pr_6O_{11} based varistor ceramics doped with different amounts of SnO_2.

based varistor ceramics consists of only two phases, ZnO and intergranular phase [7,8]. From this figure, it can be seen that in general, the doping of SnO_2 would not change the two-phase microstructure of ZnO–Pr_6O_{11} based varistor ceramics. But it should be indicated on the basis of the results of EDS analysis that some small particles, which are mainly composed of Sn and Pr, embed in ZnO grains, and larger ones, as intergranular phase, pin at ZnO grain boundaries. Combined with the results determined by XRD analysis as shown in Fig. 3, it can be concluded that the intergranular phase are mainly praseodymium oxides and $Pr_2Sn_2O_7$. Moreover, it should be indicated that on ZnO grains, small amount of Sn was also detected by EDS, indicating the doping of Sn into the ZnO grains.

The average ZnO grain size of the samples was calculated by linear intercept method from the SEM images as shown in Fig. 4. Table 1 and Fig. 5 present the calculated average ZnO grain sizes of the as-prepared ZnO–Pr_6O_{11} based varistor ceramics doped with different amounts of SnO_2. It can be clearly seen that the ZnO grain size of the samples decreases with the increase of SnO_2 doping contents. The decrease of ZnO grain size might be attributed to the formation of intergranular phase $Pr_2Sn_2O_7$ during sintering, which pins at the grain boundaries of ZnO as shown in Fig. 4, thus hindering the growth of ZnO grains [14,18].

In addition, it is noticeable that pores are clearly observed in the samples doped with SnO_2 of more than 1 mol%, and with more SnO_2 doped, the porosity increases. This result is consistent with the doping effect of SnO_2 on the relative density as illustrated in Fig. 2, and further verifies that the addition of SnO_2 acts against the sinterability of ZnO–Pr_6O_{11} based varistor ceramics.

3.3. C–V characteristics

Fig. 6 shows the *C–V* characteristics of the as-prepared ZnO–Pr_6O_{11} based varistors doped with different amounts of SnO_2. From this figure, the *C–V* characteristic parameters of the varistor samples including donor density (N_d) and barrier height (Φ_b) were calculated, and the results are illustrated in Fig. 7. Compared with the sample without SnO_2, the donor densities of all the samples doped with SnO_2, regardless of the SnO_2 doping contents, were enhanced. So, it is believed that the doped SnO_2 acts as a donor in ZnO–Pr_6O_{11} based varistors [32,33]. The barrier height of the varistors increases first and then decreases with increasing doping contents of SnO_2, in which the samples doped with 0.25 mol% and 0.5 mol% SnO_2 show relative larger barrier height than any of others. Because the increase of barrier height is in favor of the raise of varistor's nonlinear coefficient [33], so it can be expected that the samples doped with 0.25 mol% and 0.5 mol% SnO_2 would possess a relative higher nonlinear coefficient, which is consistent with the results presented in next section.

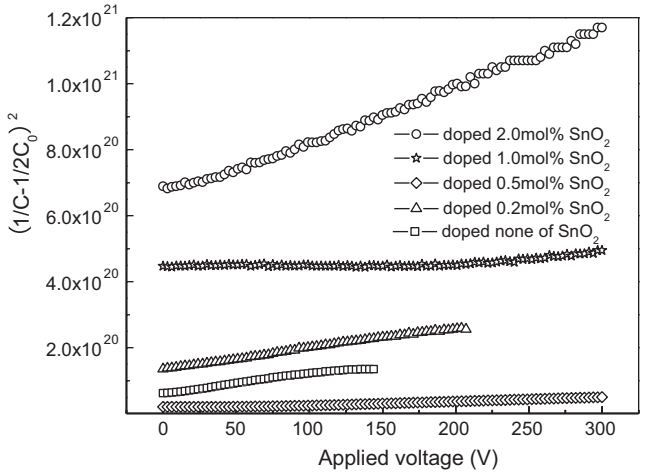

Fig. 6. The *C–V* characteristics of the as-prepared ZnO–Pr_6O_{11} based ceramic varistors doped with different amounts of SnO_2.

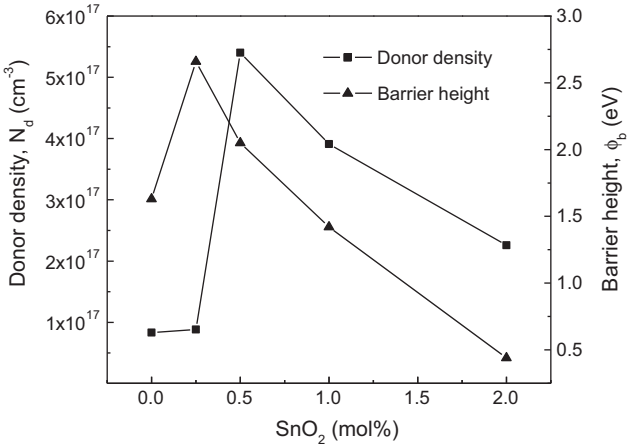

Fig. 7. The donor densities and barrier heights of the as-prepared ZnO–Pr_6O_{11} based ceramic varistors doped with different amounts of SnO_2.

3.4. E–J characteristics

The *E–J* characteristics of the as-prepared ZnO–Pr_6O_{11} based ceramic varistors doped with different amounts of SnO_2 are shown in Fig. 8. Their corresponding electrical parameters calculated from the *E–J* curves are summarized in Table 1 in detail.

From Table 1, it can be seen that the nonlinear coefficient of the ceramic varistors increases with increasing doping amounts of SnO_2, when the doping content of SnO_2 is no more than 0.5 mol%, and then the nonlinear coefficient dramatically decreases when larger amounts of SnO_2 are doped.

As the ionic radius of Sn^{4+} (0.069 nm) is smaller than that of Zn^{2+} (0.074 nm), and in the *C–V* analysis we have already known that the doped SnO_2 acts as a donor. So, it is believed that Sn^{4+} ions could replace the sites of Zn^{2+} in the lattices, which was also indirectly confirmed by EDS results as discussed in Section 3.2, and numerous electrons can be generated as carriers at the same time.

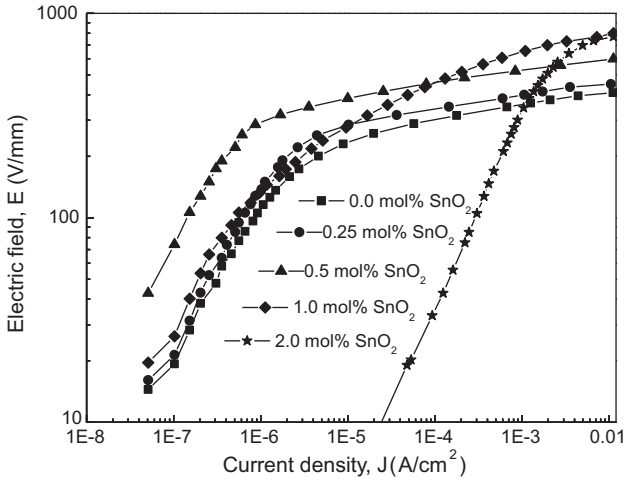

Fig. 8. The *E–J* characteristics of the as-prepared ZnO–Pr_6O_{11} based ceramic varistors doped with different amounts of SnO_2.

This substitution process can be written as follows:

$$SnO_2 \xrightarrow{ZnO} Sn_{Zn}^{\bullet\bullet} + 2e' + 2O_o^x \quad (4)$$

where, $Sn_{Zn}^{\bullet\bullet}$ is a positive charge substituted for a Zn lattice site, e' is a negative charge, and O_o^x is the neutral oxygen of an oxygen lattice site [33]. The generated carriers could improve the conductivity of ZnO grains, and this process is in favor of improving the nonlinear properties of ZnO varistors. Moreover, through the *C–V* analysis we found that the samples doped with 0.25 mol% and 0.5 mol% SnO_2 exhibited a relatively larger barrier height than the sample without SnO_2, and it is known that the increase of barrier height also plays a positive role in improving the nonlinear properties of the obtained ceramic varistors [33]. So, it can be concluded that the nonlinear coefficient of the obtained ceramic varistors would increase, when the doping contents of SnO_2 are no more than 0.5 mol%.

About the dramatic decrease in nonlinear coefficient of the obtained ZnO–Pr_6O_{11} varistors with the doping contents of SnO_2 more than 0.5 mol%, it can be explained as follows. It was reported that the degree of solid solution of tin in zinc oxide stayed below 0.1 mol % of SnO_2 and higher concentrations of SnO_2 would lead to the segregation of secondary phase [34]. After that, with further increasing amount of SnO_2 doped into the varistors, the changes of phase composition and microstructure after SnO_2 doping might play a more important role in the electrical property than the donor effect.

When the doping amounts of SnO_2 are more than 0.5 mol%, as can be seen in the XRD results presented in Fig. 3, the amount of $Pr_2Sn_2O_7$ phase generated increases apparently, and Pr_6O_{11} phase is absent because during sintering the formation of $Pr_2Sn_2O_7$ will consume Pr_6O_{11}. And, it is well-known that during sintering, Pr_6O_{11} provides for the formation of insulating boundary layers which control the operation of varistors [35]. So, it is believed that the consumption of a large number of Pr_6O_{11} by this reaction will be adverse to the formation of insulating boundary layers. Furthermore, the $Pr_2Sn_2O_7$ phase, which will segregate at grain boundary, may also destroy the insulating boundary layers. So, when the doping amounts of SnO_2 are too large, for example, more than 0.5 mol% in this case, the nonlinear coefficient of the obtained ceramic varistors may decrease.

With increasing doping amounts of SnO_2 up to 1.0 mol%, the varistor voltage of the sample increases. After that, the varistor voltage of the samples decreases when more SnO_2 is doped. The varistor voltage of ZnO–Pr_6O_{11} based varistor ceramic materials is correlated to the grain size of ZnO and the applied voltage per grain boundary [14,18]. It is in direct proportion to the applied voltage per grain boundary and inverse to the average ZnO grain size. With the increase of SnO_2 doping amounts, the increase of the varistor voltage of the samples may be mainly attributed to the decrease of their average ZnO grain size, and the decrease of the varistor voltage may be mainly owing to the abrupt decrease of the applied voltage per grain boundary of the samples when too large amount of SnO_2 is doped.

The leakage currents of the samples decrease with the increase of SnO_2 doping amounts, when the doping amounts of SnO_2 are no more than 0.5 mol%. But when the doping amount of SnO_2 is further increased, the leakage currents of the samples increase dramatically. The decrease of the leakage currents of the obtained varistor samples may be caused by the increase of their nonlinear coefficients; on the other hand, when too large amount of SnO_2 is doped, the abrupt increase of the leakage currents may be attributed to the abrupt decrease of the relative densities of the samples, in which the massively formed pores in the samples act as the hot spots for the flow of currents [1].

4. Conclusions

In ZnO–Pr_6O_{11} based varistor ceramics, the doping of SnO_2 played a role against the sinterability of the samples and the growth of ZnO grains. The average ZnO grain size decreased with the increase of SnO_2 doping contents. When the SnO_2 doping content was no more than 1.0 mol%, the varistor voltage increased with increasing amount of SnO_2 doped. The doped SnO_2 acted as donor in ZnO–Pr_6O_{11} based varistors, and minor doping of SnO_2 up to 0.5 mol% can improve the nonlinear coefficient and reduce the leakage current of the ceramic varistors.

Acknowledgements

The authors would like to thank the financial support for this work from Scientific Research Foundation for Returned Overseas Chinese Scholars sponsored by State Education Ministry, the National Natural Science Foundation of China (grant no. 60806005), the Transfer and Industrialization Project of Sci-Tech Achievement (Cooperation Project between University and Factory) sponsored by Beijing Municipal Commission of Education, and State Key Laboratory of New Ceramic and Fine Processing, Tsinghua University (grant No. KF0903).

References

[1] T.K. Gupta, J. Am. Ceram. Soc. 73 (1990) 1817–1840.
[2] S. Fujitsu, H. Toyoda, H. Yanagida, J. Am. Ceram. Soc. 70 (1987) C71–C72.
[3] D.R. Clarke, J. Am. Ceram. Soc. 82 (1999) 485–502.
[4] P.R. Bueno, J.A. Varela, E. Longo, J. Eur. Ceram. Soc. 28 (2008) 505–529.
[5] Y.S. Lee, T.Y. Tseng, J. Am. Ceram. Soc. 75 (1992) 1636–1640.
[6] C.W. Nahm, Mater. Lett. 57 (2003) 1317–1321.
[7] K. Mukae, Am. Ceram. Soc. Bull. 66 (1987) 1329–1331.
[8] K. Mukae, K. Tsuda, S. Shiza, IEEE Trans. Power Delivery 3 (1988) 591–598.
[9] C.W. Nahm, J. Am. Ceram. Soc. 93 (2010) 3056–3059.
[10] C.W. Nahm, Ceram. Int. 37 (2011) 265–271.
[11] H.K. Varam, K.P. Kumar, K.G.K. Warrier, A.D. Damodaran, J. Mater. Sci. Lett. 8 (1989) 974–976.
[12] C.W. Nahm, J. Am. Ceram. Soc. 93 (2010) 2297–2304.
[13] H. Feng, Z.J. Peng, X.L. Fu, Z.Q. Fu, C.B. Wang, L.H. Qi, H.Z. Miao, J. Alloys Compd. 497 (2010) 304–307.
[14] C.W. Nahm, Mater. Sci. Eng. B 170 (2010) 123–128.
[15] J. Hu, J.L. He, W.C. Long, J. Liu, J. Am. Ceram. Soc. 93 (2010) 2155–2157.
[16] C.W. Nahm, J. Mater. Sci. 40 (2005) 6307–6309.
[17] Z.J. Peng, X.L. Fu, Y.X. Zang, Z.Q. Fu, C.B. Wang, L.H. Qi, H.Z. Miao, J. Alloys Compd. 508 (2010) 494–499.
[18] C.W. Nahm, Ceram. Int. 36 (2010) 1495–1501.
[19] H.H. Hng, K.M. Knowles, J. Mater. Sci. 37 (2002) 1143–1154.
[20] C.W. Nahm, J. Eur. Ceram. Soc. 21 (2001) 545–553.
[21] F.H. Liu, G.J. Xu, L. Duan, Y.L. Li, Y. Li, P. Cui, J. Alloys Compd. 509 (2011) L56–L58.
[22] M. Peiteado, Y. Iglesias, A.C. Caballero, Ceram. Int. 37 (2011) 819–824.
[23] C.W. Nahm, J. Alloys Compd. 505 (2010) 657–660.

[24] D. Xu, X.N. Cheng, G.P. Zhao, J. Yang, L.Y. Shi, Ceram. Int. 37 (2011) 701–706.
[25] K.Y. Yuan, G.R. Li, L.Y. Zheng, L.H. Cheng, L. Meng, Z. Yao, Q.R. Yin, J. Alloys Compd. 503 (2010) 507–513.
[26] C.W. Nahm, J. Alloys Compd. 490 (2010) L52–L54.
[27] M. Takada, S. Yoshikado, Key Eng. Mater. 350 (2007) 213–216.
[28] S. Bernik, N. Daneu, J. Eur. Ceram. Soc. 21 (2001) 1879–1882.
[29] N. Daneu, A. Recnik, S. Bernik, D. Kolar, J. Am. Ceram. Soc. 83 (2000) 3165–3171.
[30] Z.J. Peng, C.B. Wang, L.J. Gauckler, H.Z. Miao, Key Eng. Mater. 368–372 (2008) 479–482.
[31] X.L. Fu, W.H. Tang, Z.J. Peng, Acta Phys. Sin. 57 (2008) 5844–5852.
[32] K. Mukae, K. Tsuda, I. Nagasawa, J. Appl. Phys. 50 (1977) 4475–4476.
[33] J.A. Park, Physica B 403 (2008) 639–643.
[34] M. Peiteado, Y. Iglesias, J. De Frutos, J.F. Fernandez, A.C. Caballero, Boletin De La Sociedad Espanolade Ceramica Y Vidrio. 45 (2006) 158–162.
[35] B.S. Skidan, M.M. M'int, Glass Ceram. 64 (2007) 31–33.